Synthesis of Poly(styrene−dimethylsiloxane) Block Copolymers: Influence of the Phase-Separated Morphologies on the Thermal Behaviors

David Rosati, Michel Perrin, and Patrick Navard*

Centre de Mise en Forme des Matériaux, Ecole des Mines de Paris, UMR CNRS 7635, BP 207, F-06904 Sophia-Antipolis, France

Valeria Harabagiu and Mariana Pinteala

"P. Poni" Institute of Macromolecular Chemistry, Aleea Gr. Ghica Voda 41 A, 6600 Jassy, Romania

Bogdan C. Simionescu

Department of Macromolecules, "Gh. Asachi" Technical University, 6600 Jassy, Romania

Received October 28, 1997; Revised Manuscript Received April 17, 1998

ABSTRACT: Five polystyrene−poly(dimethylsiloxane) di- and triblock copolymers were prepared by two different methods, a classical anionic polymerization and a cationic polymerization of styrene in the presence of a new macromolecular initiator. Spherical, cylindrical, and lamellar phase-separated morphologies were identified. Their sizes were measured by transmission electron microscopy (TEM) on films obtained from bulk and solvent-cast samples. DSC and TEM show that the phase-separated morphologies are strongly segregated with no long range ordering. The specific microphase surface area, obtained by TEM, is strongly correlated with the broadening of the polystyrene glass transition.

Introduction

Flexible noncrystalline di- (AB) and triblock (ABA) copolymers are well-known to form various distinct periodic phase-separated morphologies or microphases (usually spheres, cylinders, and lamellae) as either the temperature is lowered or the molecular weight is increased.[1] Whatever the degree of segregation, the different types of ordered states depend mainly on the composition, the statistical segment length asymmetry, the overall degree of polymerization N, and the quench parameter (χN), χ being the Flory interaction parameter.[2−4] From a mean-field theory, Leibler predicted that the order-to-disorder transition (ODT) in diblock copolymer melts is weakly first order, except for symmetric diblocks.[2] Fredrickson and Helfand showed in a subsequent paper[3] that the ODT for perfectly symmetric diblocks is also weakly first order, due to the occurrence of large-amplitude concentration fluctuations not considered in the mean-field approach of Leibler. More recently, the density functional approach of Muthukumar predicts ranges in compositions for a direct transition between the disordered state and any of the ordered states. This seems to be consistent with experimental results.[5,6]

Over the last few years, polystyrene/poly(dimethylsiloxane) (PS/PDMS) block copolymers have been studied for their potential technological importance, as thermoplastic elastomers and as materials resistive to oxygen reactive ion etching and for their unusual physical properties. Di-, tri-, and multiblock siloxane-containing copolymers have been prepared by different synthetic approaches, like (1) living anionic polymerization of nonpolar vinyl and diene compounds with cyclic siloxanes,[7−10] (2) polyaddition of α,ω-dihydro-terminated polysiloxane to α,ω-divinyl-terminated polymers,[11.12] and (3) incorporation of easily cleavable linkages in polysiloxane chains in order to convert them into potential macroinitiators and their further use in radical polymerization of vinyl monomers.[13−16] Their unusual behavior as compared to the corresponding styrene/diene block copolymers has already been noticed. (a) For microphase-separated samples, no depression of the PS glass transition temperature has been noticed, compared with that of the corresponding homopolystyrene, since the PS blocks have a sufficiently high molecular weight (≥10 000).[17] (b) Although standard spherical, cylindrical, and lamellar morphologies have been identified mainly by small angle X-ray scattering (SAXS), a significant lack of coherent order in the microstructures has been systematically noticed.[6,8,9,18] (c) Moreover, due to the pronounced incompatibility between these two chemical species, no one has succeeded in reaching experimentally the order-to-disorder transition without going first through the thermal decomposition. This renders the thermodynamical equilibrium morphology difficult to attain. Neither has it been possible to estimate with precision the Flory interaction parameter, using small angle X-ray (SAXS) or neutron scattering (SANS), and no experimental phase diagram has been built. (d) In addition, the strongly segregated part of the phase diagram seems to be skewed in the direction of the low styrene content.[6] This cannot be explained taking into account the current statistical segment length asymmetry corrections. Because of experimental difficulties, there has been no systematic report on the direct observation by transmission electron microscopy (TEM) of the poly(S-*b*-DMS) phase-separated morphologies. Furthermore, the few DSC investigations of these block copolymers[6,17] have not been able to clearly relate the thermal peculiarities, like the broadening of the T_g, to

* To whom correspondence should be addressed.

S0024-9297(97)01577-5 CCC: $15.00
Published on Web 06/09/1998

the phase-separated morphologies.

The objectives of this paper are first to prepare poly(S-*b*-DMS) and poly(S-*b*-DMS-*b*-S) by a new polymerization method, and then to study and compare their morphological and thermal properties.

Experimental Section

Materials and Molecular Characterization. Cyclosiloxane monomers were dried over calcium hydride and distilled in an argon atmosphere. The coupling agents, chlorotrimethylsilane and dichlorodimethylsilane, were distilled under argon. Styrene was treated with 10% sodium hydroxide solution, washed with water, dried over calcium hydride, and distilled under vacuum just before use. The 1,4,7,10,15-pentaoxacyclopentadecane (15-C-5) was dried by azeotropic distillation of water in the presence of benzene and by heating at 30° C in a high vacuum, for 24 h. All solvents (benzene, tetrahydrofuran, chloroform) were purified according to standard methods.

^{1}H-NMR spectroscopy was performed on a Bruker 250 MHz spectrometer. Average molecular weights were measured by GPC (Waters Associated 440 apparatus, equipped with a R 401 differential refractometer and with μ-Styragel columns, calibration being made with polystyrene standards). Toluene was used as solvent.

Synthesis. (Chloromethyl)phenethyl-terminated poly(dimethylsiloxane) (Cl-PDMS-Cl) (M_n(GPC) = 1610; M_w/M_n(GPC) = 1.67; chlorine content = 4.15% by weight; substitution degree = 96%) was prepared through a two-step procedure described previously.[19] Firstly, the hydrosilation of styrene with hydride-terminated poly(dimethylsiloxane) (concentration, 50% by weight in toluene) was performed in the presence of a H_2PtCl_6 catalyst, at 100 °C. In a second step, the aromatic rings (Ph) attached to the siloxane chain in final positions were chloromethylated in mild conditions (0−20 °C; 8 h) with the paraformaldehyde/trimethylchlorosilane/$SnCl_4$ system (CH_2O/$(CH_3)_3SiCl/SnCl_4$ = 1/1/0.14 molar ratio) in chloroform ([CH_2O] = 8 mol/L; CH_2O/Ph = 8 molar ratio).

Cationic polymerization of styrene (S) in the presence of the Cl-PDMS-Cl/$SnCl_4$ macromolecular initiator was performed in chloroform at 20 °C, under argon. The solvent, the siloxane precursor ([$PhCH_2Cl$] = 0.04 mol/L), and $SnCl_4$ ($SnCl_4/PhCH_2Cl$ = 4 molar ratio) were introduced into the reaction flask under argon and stirred for 15 min. Then the monomer ($[S]_0$ = 0.40 mol/L) was added with a dry syringe. The reacting mixture turned red, and it was subsequently stirred vigorously for a period of 8 h. The polymerization was stopped by adding a large volume of a mixture of methanol/10% $NaHCO_3$ aqueous solution (9/1 v/v). The poly(S-*b*-DMS-*b*-S) triblock copolymer was recovered by filtration. The unreacted polysiloxane was extracted with petroleum ether and the polystyrene homopolymer was removed by its precipitation in a cyclohexane/*n*-heptane mixture. The purified triblock T90 (see Table 1) was obtained in a 91.3% yield.

Sequential anionic polymerization of styrene and hexamethylcyclotrisiloxane was carried out under argon in a reaction vessel equipped with a magnetic stirrer, a reflux condenser, and a three-way stopcock. The calculated amounts of benzene, tetrahydrofuran (THF) (benzene/THF = 20/1 v/v), and styrene ($[S]_0$ = 15% by weight) were introduced by the syringe technique into the reaction vessel. The mixture was frozen and degassed several times under a high vacuum. The BuLi initiator was added at 0 °C and a red living polystyrene was observed. The polymerization of styrene was carried out at this temperature for 1 h. A small aliquot of the reaction mixture was then extracted by syringe and precipitated into methanol to determine the molecular weight of the polystyrene sequence. A solution of complexing agent (15-C-5) in THF (concentration 10% by weight; BuLi/15-C-5 = 1/1 molar ratio) was then added to increase the reactivity of the anionic macromolecular species. Hexamethylcyclotrisiloxane monomer was then slowly introduced as a solution in THF (30% by weight) into the reaction vessel, and the temperature was increased to 50 °C. The red color disappeared by the transformation of the polystyryl active species into a siloxanolate growing chains. After 4 h of stirring at this temperature, the reaction was stopped with trimethylchlorosilane or with dimethyldichlorosilane (BuLi/SiCl = 1/1.2 molar ratio) to prepare poly(S-*b*-DMS) diblock or poly(S-*b*-DMS-*b*-S) triblock copolymers, respectively. After a purification procedure similar to that used for the cationically obtained copolymer, the diblock samples D51 and D63 and the triblock samples T50 and T82 (see Table 1) were obtained in 90−93% yields.

Differential Scanning Calorimetry. Differential scanning calorimetry (DSC) measurements were carried out using a Perkin-Elmer DSC7 calibrated with indium. Low-temperature scans were performed by Dr. M. F. Achard in Bordeaux. Before each experiment, the base line was carefully determined in order to correct the data. Samples were quenched from room temperature at the maximum cooling rate (−320 °C·min^{-1}) down to −150 °C and then scanned at 10 °C·min^{-1} from −135 up to +150 °C. Four subsequent scans were performed at 10 °C·min^{-1} for each sample. There was no waiting time between each run and the cooling rate was −10 °C·min^{-1}. The glass transition temperatures T_g, the change in specific heat Δc_p, and the width of the glass transition region ΔT_g were determined by a standard method extrapolating the linear portion of DSC traces.[17] In the following, $T_{g,PDMS}$, $T_{g,PS}$, $\Delta c_{p,PS}$, $T_{g,mix}$, and $\Delta c_{p,mix}$ are the glass transition temperatures of PDMS microphases, the glass transition temperatures and the change in specific heat of PS microphases and of disordered (isotropic) sample, respectively. The values of $\Delta c_{p,PS}$, evaluated for PS microphases, are quoted per gram of PS blocks for comparison with homopolystyrene. $T_{C.C}$ and T_m correspond to the temperature of cold crystallization and melting processes in the PDMS microphases, respectively. The measured DSC data (see Table 2) are averaged on the three last subsequent scans, except for $T_{C.C}$ and $T_{g,PDMS}$.

Transmission Electron Microscopy. Samples for transmission electron microscopy (TEM) were prepared either by solvent casting on a Teflon surface using neutral solvents such as toluene and chloroform[6,9,18] or by direct means with the copolymer powder on the carbon-coated copper grid. This has been done in order to avoid the difficulties that were experienced with microtomes. Thin films (≤50 nm) were annealed around 5 days at 110 °C under vacuum and quenched at room temperature from 100 °C. Due to the PS glass transition (see below), we think the observed morphologies are near those encountered at 100 °C. The high electron density of PDMS microphases as compared to PS gave sufficient contrast without the need of staining. Samples were examined using a Philips CM12 transmission electron microscope operating at 120 kV, the copolymers being relatively stable under such an accelerating voltage. On the TEM bright-field pictures, PDMS microdomains appear black.

Results

Synthesis. The styrene/siloxane molar ratios, molecular weights, styrene weight fraction, apparent block copolymer polydispersity, and decomposition temperature are listed in Table 1. Samples are simply designated by "D" or "T" for di- or triblock followed by the molar percentage of styrene. The styrene/siloxane molar ratios in block copolymers were calculated from specific proton integrals (δ = 0.1 ppm, 6 p, CH_3−(Si); δ = 1.3−2.0 ppm, 3 p, −CH_2−CH(Ph); δ = 6.5−7.2 ppm, 5 p, Ph) by ^{1}H-NMR spectroscopy. Block copolymer molecular weights M_n are calculated from styrene/siloxane molar ratios (see Table 1 captions). The weight average molecular weight, M_w, was determined using the GPC-determined apparent block copolymer polydispersity.

DSC. DSC results presented in Figures 1 and 2 and Table 2 provide a qualitative indication of the block copolymer phase states. On the second, third, and fourth scans, samples T50, D51, D63, and T82 exhibit

Table 1. Molecular Characterization of the PS/PDMS Block Copolymer Samples

samples	styrene/-siloxane molar ratio[a]	M_n of S blocks	M_n	M_w/M_n[b]	styrene weight fraction	dec temp[e] (°C)
D51	1.05	8 100[b]	13 600[c]	1.20	0.60	265
D63	1.68	8 200[b]	11 700[c]	1.15	0.70	250
T50	1.00	8 100[b]	27 800[c]	1.09	0.58	280
T82	4.49	6 900[b]	16 000[c]	1.10	0.86	260
T90	8.78	8 200[d]	17 700	1.46	0.93	255

[a] Determined by ^{1}H NMR. [b] Determined by GPC. [c] Calculated according to

$$M_n = (M_n \text{ of S block})\left(1 + \frac{1}{\alpha(\text{styrene/siloxane molar ratio})}\frac{74.13}{104.15}\right)$$

with $\alpha = 1$ for the diblocks and $\alpha = 1/2$ for the triblocks. [d] Calculated according to

$$M_n = (M_n \text{ of PDMS block}) \times \left(1 + 0.5(\text{styrene/siloxane molar ratio})\frac{104.15}{74.13}\right)$$

. [e] Beginning of thermal decomposition (determined by thermogravimetry analysis).

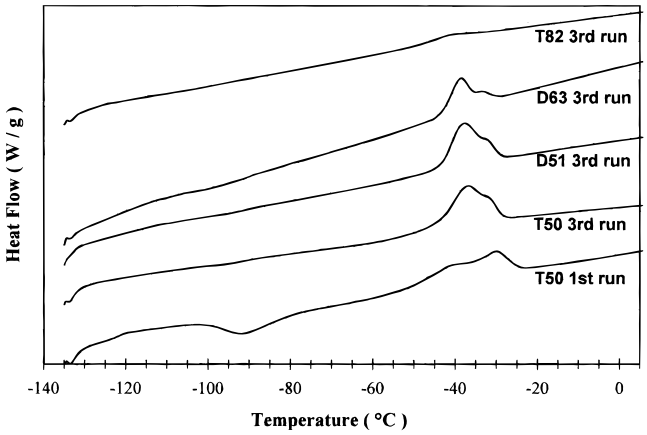

Figure 1. Low-temperature DSC heating trace of the phase-separated PS/PDMS block copolymers. Curves are vertically shifted for presentation. The bottom curve is from the first run conducted on the T50 sample. The four other curves are from the third run conducted on T50, D51, D63, and T82. T90 (not shown) does not exhibit any event at low temperature.

two principal features, the PDMS phase melting endotherm near −38 °C and the PS phase glass transition near 90 °C. In addition, on the first run these four samples exhibit both a PDMS cold crystallization exotherm near −90 °C and the PDMS phase glass transition $T_{g,PDMS}$ at −123 °C, due to the quench procedure. These two features are absent on subsequent runs.

As Krause et al. and Chu et al.[6,17] had already noticed for similar samples, the areas of the melting endotherms are larger than the corresponding exotherm, which means that the glass transition measured for the PDMS phase corresponds to a partially crystalline material. The remaining triblock, T90, is characterized on the four runs by a single glass transition, at an intermediate temperature of 69 °C. Thus the T50, D51, D63, and T82 block copolymers are microphase-separated up to at least their $T_{g,PS}$.

On the contrary, T90 seems to be disordered up to 69 °C. The approximate rule of Gordon and Taylor[20] can be used to estimate the $T_{g,mix}$ of the "disordered" triblock T90 (thermally equivalent to a random copolymer

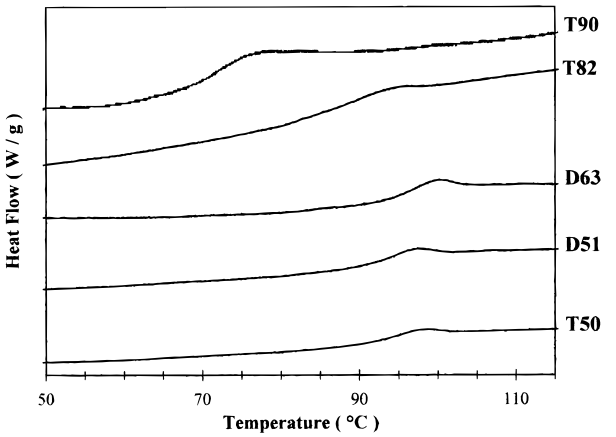

Figure 2. High-temperature heating trace of the five PS/PDMS block copolymers. Curves are vertically shifted for presentation. The curves are from the third run conducted on each of the samples. T90 exhibits a T_g event at a lower temperature because it is the glass transition of a disordered PS/PDMS phase.

having the same weight composition)

$$T_{g,mix} = \frac{w_{PS}T_{g,PS} + Kw_{PDMS}T_{g,PDMS}}{w_{PS} + Kw_{PDMS}} \quad (1)$$

where w_{PS} and w_{PDMS} are the weight fractions of the two species and K is a constant close to unity. For a given pair, K can be calculated from the thermal expansivities of the corresponding homopolymers

$$K = \frac{\alpha_r^{PDMS} - \alpha_g^{PDMS}}{\alpha_r^{PS} - \alpha_g^{PS}} \quad (2)$$

where the subscripts g and r refer to the glassy and the rubbery states, respectively. With the corresponding homopolymer values, $T_{g,PDMS} = -123$ °C[21] and $\alpha_r^{PDMS} - \alpha_g^{PDMS} \approx 5.7 \times 10^{-4}$ K^{-1} [22] for PDMS and $T_{g,PS} = 93$ °C (see Table 3) and $\alpha_r^{PS} - \alpha_g^{PS} \approx 3.7 \times 10^{-4}$ K^{-1} [21] for PS, a $T_{g,mix}$ of 68 °C is obtained, which is in good agreement with the measured value. Figure 2 gives a comparison of the four $T_{g,PS}$ values of T50 D51, D63, and T82 with the $T_{g,mix}$ of T90. Table 3 gives the thermal properties of the PS microphases as compared to those of a similar molecular weight homopolystyrene. The predicted homopolymer glass transition temperatures are obtained by fitting with Krause data[17] the Flory−Fox equation,[23] giving $T_g(M_n) = 378 + 9.63 \times 10^{-4}/M_n$, for a heating rate of 10 °C·min^{-1}. All measured $T_{g,PS}$ values for the phase-separated samples are close to the corresponding homopolymer-predicted glass transition temperature $T_{g,PS}^{homo}$, except for that of T82, which is 6 °C lower. Table 3 also gives the $1 - (\Delta c_{p,PS}/\Delta c_{p,PS}^{homo})$, ratio which provides a weight fraction estimate of the amount of PS chain segments that do not take part in the PS microphase glass transition.[24] To estimate this ratio, the specific heat change at the glass transition of homopolystyrene $\Delta c_{p,PS}^{homo}$ has been taken as 0.288 J·K^{-1}·g^{-1}, which is a typical averaged value extracted from the literature.[17] For our microphase-separated samples this ratio is less than 3%. There is no significant phase mixing, as expected for strongly segregated block copolymers with sharp microphase boundaries (see Discussion). As already mentioned,[25,26] the most striking difference between the copolymer glass transitions and those of the corresponding ho-

Table 2. Thermal properties of the Five PS/PDMS Di- and Triblock Copolymers

samples	$T_{g,PS}$[a] (°C)	$\Delta C_{p,PS}$[b] ($J \cdot g_{PS}^{-1} \cdot K^{-1}$)	$\Delta T_{g,PS}$[c] (°C)	$T_{g,mix}$[d] (°C)	$\Delta C_{p,mix}$[e] ($J \cdot g^{-1} \cdot K^{-1}$)	$\Delta T_{g,mix}$[f] (°C)	T_m[g] (°C)	$T_{C.C}$[h] (°C)	$T_{g,PDMS}$[i] (°C)
D51	91	0.286	11				−38	−90	−123
D63	93	0.296	14				−38	−93	−123
T50	92	0.284	10				−37	−90	−123
T82	85	0.279	16				−40		−123
T90				69	0.687	11			

[a] PS glass transition temperature. [b] PS specific heat change. [c] PS glass transition width. [d] PS/PDMS disordered phase glass transition temperature. [e] PS/PDMS disordered phase specific heat change. [f] PS/PDMS disordered phase glass transition width. [g] PDMS melting temperature. [h] PDMS cold crystallization temperature. [i] PDMS glass transition temperature.

Table 3. Homopolymer/Block Copolymer Thermal Behavior Comparison

samples	$T_{g,PS}^{homo}$[a] (°C)	$T_{g,PS}^{homo} - T_{g,PS}$ (°C)	$\Delta T_{g,PS}/T_{g,PS}$	$1 - (\Delta C_{p,PS}/\Delta C_{p,PS}^{homo})$ (%)
D51	93	2	0.030	0.7
D63	93	0	0.038	very small
T50	93	1	0.027	1.4
T82	91	6	0.045	3.0
T90	93			

[a] Homopolystyrene glass transition temperature as calculated from the Flory−Fox equation.

Table 4. Morphological Characterization of the PS/PDMS Block Copolymers

samples	$N_{n,PS}$[a]	N_n[b]	$f = N_{n,PS}/N_n$	ϕ_{PS}[c] (100 °C)	microstructure (at 110 °C)	microdomains size (nm)	$10^{-4} \cdot S$ ($m^2 \cdot kg^{-1}$)	χN (at 100 °C)
D51	78	152	0.51	0.56	lamellae	31 ± 3[e]	6.5	43
D63	79	126	0.63	0.67	PDMS cylinders	30 ± 3[d]	13.0	36
T50	156	312	0.50	0.55	lamellae	42 ± 5[e]	4.6	44[f]
T82	133	163	0.82	0.85	PDMS spheres	11 ± 3[d]	53.1	23[f]
T90	158	176	0.90	0.92	disordered			

[a] PS block number average degree of polymerization. [b] Overall degree of polymerization. [c] PS volume fraction. [d] Apparent microdomain diameter. [e] Apparent lamellar periodicity. [f] For triblock N_n has been taken as $N_{n,PS}/2 + N_{n,PDMS}/2$ for comparison with diblock.

mopolymers lies in the $\Delta T_g/T_g$ ratio, which represents the relative width of the glass transition region. In our case, the copolymer ratios associated with PS microphases are almost twice that of the corresponding homopolymer one, which is near 0.0016.[17]

Electron Microscopy. We were able to obtain good electron microscopy images from the five block copolymers quenched from 100 °C. The types of microstructure and their mean dimensions were obtained. The results are reported in Table 4. The degrees of polymerization, N_n , were estimated from number average molecular weight data. The PS volume fractions, ϕ_{PS}, were estimated using the monomer specific volume Fox empirical equations for PS and PDMS homopolymer[27]

$$v_{PS} = 0.767 + 5.5 \times 10^{-4}T + 643 \times 10^{-4}(T/M_n) \quad (cm^3 \cdot g^{-1}) \quad (3)$$

$$v_{PDMS} = 0.672 + 12 \times 10^{-4}T + 1550 \times 10^{-4}(T/M_n) \quad (cm^3 \cdot g^{-1}) \quad (4)$$

at 100 °C. We have neglected in this estimate the presence of any interfacial volume or interphase. Because our microphase-separated block copolymers are strongly segregated, it is impossible to prepare samples by quenching from the disordered state, making it difficult to be certain that the morphologies obtained directly from the powders are equilibrium ones. Thus, considering the previous conclusion of Bajaj and Varshney,[9] Chu et al.,[6] and Chen et al.,[18] who established that toluene and chloroform are neutral solvents for the PS/PDMS system, TEM examinations were all conducted on films cast from toluene and chloroform in order to approach the equilibrium morphology as closely as possible. The D51 and T50 samples cast from toluene show poorly oriented lamellae microstructures, as evidenced in Figure 3 for D51. The apparent periodicities were estimated at 31 ± 3 nm for D51 and 42 ± 5 nm for T50. The bulk samples examined directly from the powder show a qualitative agreement, but due to a poor contrast it was difficult to perform any periodicity measurement. D63, shown in Figure 4, exhibits a rodlike structure of PDMS in a PS matrix, which does not seem to be hexagonally packed as for standard styrene/diene block copolymers.[1−5] The apparent cylinder diameter is 30 ± 3 nm. The bulk sample shows

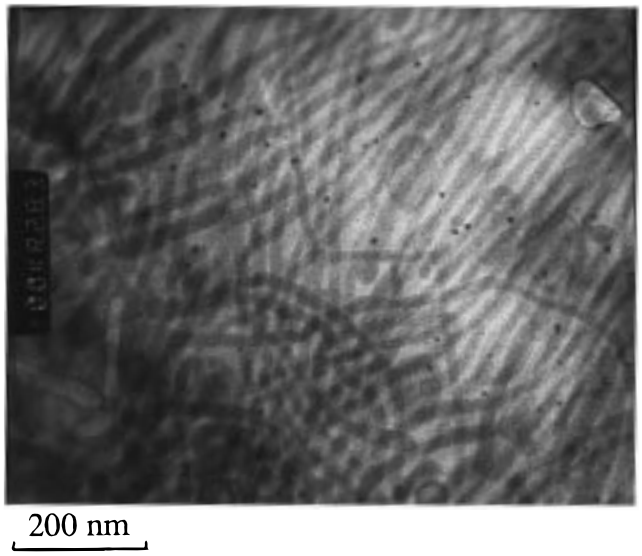

Figure 3. TEM image of D51 sample cast from toluene on Teflon. The PDMS lamellae appear black. The apparent periodicity is 31 ± 3 nm. T50 (not shown) has exactly the same morphology with a periodicity of 42 ± 5 nm.

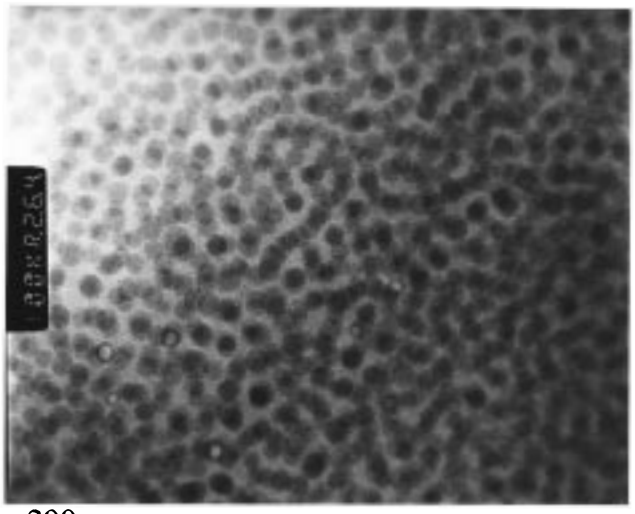

Figure 4. TEM image of sample D63 cast from toluene on Teflon. A PDMS rodlike structure in a PS matrix appears black. The cylinders' apparent diameters are 30 ± 3 nm.

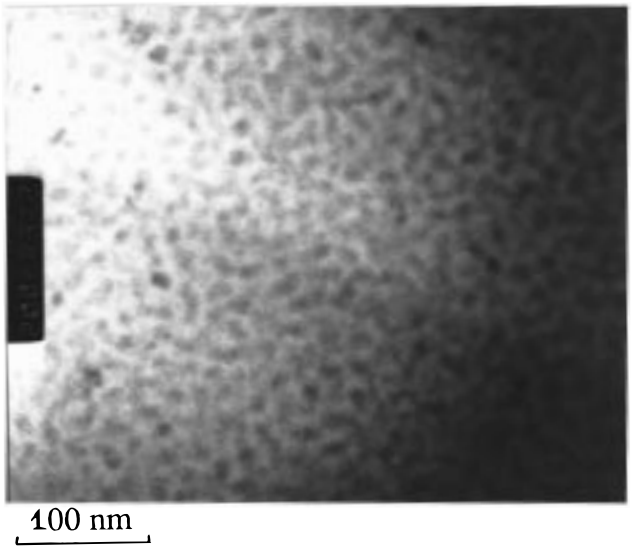

Figure 5. TEM image of sample T82 cast from toluene on Teflon. PDMS spheres in a PS matrix appears black. The spheres' apparent diameters are 11 ± 3 nm.

the same morphology. Optical observations (from depolarized optical microscopy and small angle light scattering experiments) confirm the lamellae and cylindrical microstructures of T50, D51, and D63, respectively.[28] T82, in Figure 5, clearly exhibits a spherical microstructure of PDMS spheres randomly distributed in a PS matrix. The apparent sphere diameter was estimated to be 11 ± 3 nm. Again the same qualitative agreement is obtained with the bulk morphology. Finally, T90 appears disordered (not shown). Exactly the same morphologies were identified for each of the five samples cast from chloroform.

For all microphase-separated samples, the specific surface (see Discussion)

$$S = \left(\frac{\text{microdomain surface}}{\text{microdomain volume}}\right) v_{PS} \qquad (m^2 \cdot kg^{-1}) \quad (5)$$

has been estimated using TEM microdomain size estimation (see Table 4).

Discussion

Synthesis. Five well-defined poly(S-*b*-DMS) and poly(S-*b*-DMS-*b*-S) di- and triblock copolymers were synthesised by two different approaches: a new cationic polymerization of styrene in the presence of the organochlorofunctional poly(dimethylsiloxane)/$SnCl_4$ system and a modification of a classical anionic polymerization of styrene initiated by butyllithium, followed by subsequent polymerization of hexamethylcyclotetrasiloxane in the presence of polystyryllithium/15-C-15 active species.

The cationic polymerization of styrene in the presence of the siloxane macromolecular bifunctional cationic initiator (see structure below) proved to be a useful new method in the preparation of poly(S-*b*-DMS-*b*-S) triblock

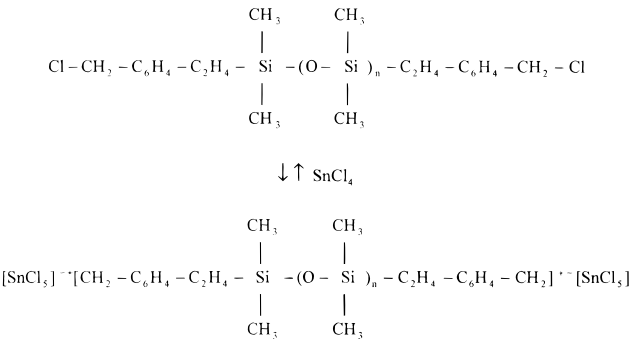

copolymers having PDMS as the central sequence. Chloromethyl-terminated poly(dimethylsiloxane) (Cl-PDMS-Cl) was prepared through a procedure previously described[19] by the chloromethylation of end-phenethyl groups attached to the siloxane chain, in mild conditions with the paraformaldehyde/trimethylchlorosilane/$SnCl_4$ mixture. The polymerization of styrene was initiated by the Cl-PDMS-Cl/$SnCl_4$ system. To check for any possible interactions between the cationic active species and the polysiloxane chain,[29] a solution of benzyl chloride (BC), $SnCl_4$ (BC/$SnCl_4$ = 4.0 molar ratio), and octamethylcyclotetrasiloxane in CH_2Cl_2 ($[BC]_0$ = 0.04 mol/L and $[\text{octamethylcyclotetrasiloxane}]_0$ = 0.40 mol/L) was stirred at 20 °C for 24 h. No evidence of the polymerization of octamethylcyclotetrasiloxane in a carefully dried system was observed by gas chromatography and GPC: only octamethylcyclotetrasiloxane cycles were detected in the product obtained after quenching of the active species with a mixture of methanol/10% $NaHCO_3$ aqueous solution, washing the organic phase with water, drying, and evaporating the solvent. As the siloxane bonds in octamethylcyclotetrasiloxane and in a linear siloxane behave similarly to electrophilic attack,[30] the pertinent conclusion is that the siloxane chain remained untouched during the cationic process. In these conditions, the molecular weight of the siloxane sequence is imposed by the reaction parameters of the preparation of the Cl-PDMS-Cl prepolymer, while the molecular characteristics of the polystyrene component and of the block copolymer are determined by the step of cationic polymerization of the vinyl monomer (active species and styrene concentrations, solvent nature, temperature, reaction time). The structure and the molecular characteristics of the Cl-PDMS-Cl bifunctional prepolymer were established by ^{1}H-NMR, chemical analysis (chlorine content), and gel permeation chromatography. Starting from a Cl-PDMS-Cl bifunctional prepolymer, a triblock copoly-

mer (sample T90) was obtained in good yield. Even though the functionality of chlorofunctional siloxane precursor was slowly lower than 2, the possible resulting diblock copolymer was not observed by GPC analysis of the final product (the GPC curve is monomodal and symmetrical, and the polydispersity index is quite low).

Physical Properties. The physical properties of the five di- and triblock copolymers that have been examined fall in two general categories. T90 exhibit random copolymer-like thermal behavior from −135 °C up to +150 °C, which indicates that the order-to-disorder transition temperature may be below $T_{g,mix}$ (as discussed below). Such a specific behavior has already been seen by Sthün[31] for a PS/PMMA diblock copolymer. T50, D51, D63, and T82 exhibit microphase-separated block copolymer-like behavior from −135 °C up to +150 °C, which indicates that the order-to-disorder temperature is at least above $T_{g,ps}$.

In weakly (for $\chi N \leq 12.5$) and intermediate segregated regimes (for $12.5 \leq \chi N \leq 50-100$),[4,32] due to moderate block incompatibility, block copolymer microstructures are supposed to have an extended interface. These are defined by a nonsaturated ordered-state composition profile, which does not disappear up to the strongly segregated regime (as χN values approach roughly 50−100). Considering the small amount of PS block segments (∼1%) that do not participate in the glass transition process (see Table 2), T50, D51, and D63 block copolymers are expected to be very strongly segregated with well-defined interfaces and nearly pure microdomains up to 150 °C. In fact, rheological measurements of storage and loss modulus have shown that up to the thermal-induced polymer decomposition around 250 °C (see Table 1), D63, D51, and T50 are microphase-separated with $G' \sim G''$ in the terminal zone behavior and scaling with ω.[0.4−0.6 33] Without any accessible order to disorder transition, it is impossible to perform any precise measurement of the associated Flory interaction parameters using SAXS (or SANS) experiments.[34] Sthün's work suggests a strong dependence of χ on the PS volume fraction ϕ_{PS}[31] and Mori et al.'s work a dependence on the polydispersity index.[35] Nevertheless, a rough estimate may be obtained using PS and PDMS solubility parameters,[21] giving $\chi \approx 106/T$, which is of the same order as existing data.[36] As an illustration, using Sthün's results for $\phi_{PS} = 0.5$,[31] the quench parameter estimated at 100 °C for D51 (see Table 4) is roughly 4 times the corresponding styrene/isoprene parameter. Such simple arguments may explain why PS/PDMS block copolymers exhibit such strongly segregated thermal behavior as compared with other block copolymers. The χN estimate of 23 for T82 (see Table 4) indicates that this sample lies in the intermediate segregated regime at the PS microphase glass transition. T90 is believed to be always in a disordered state because its order-to-disorder transition temperature is expected to be lower than $T_{g,mix}$. Indeed, from the triblock generalized Leibler theory,[2,37] a value of 55.37 is obtained for $(\chi N)_s$, the spinodal quench parameter. In this calculation, the influence of the polydispersity and the statistical segment length asymmetry have been taken into consideration, following the correction proposed by Mori et al.[35] Thus, a rough estimate of 64 °C for the order-to-disorder temperature may be proposed from the $(\chi N)_s$ calculated value (with $\chi \approx 106/T$ and $N = 176$), which is lower than $T_{g,mix} \approx 68-69$ °C. Despite that no phase diagram could be drawn for the PS/PDMS system, Winey et al.'s experimental phase diagram, constructed for PS/PI diblock copolymers,[5] predicts the good morphology for D51, D63, T50, and T82. Thus, we note here a difference with the previous Chu et al. results,[6] indicating that the PS/PDMS phase diagram for a diblock is more skewed toward the low styrene volume fraction than those constructed for PS/PI. D51, which has the same volume fraction as the 59 sample studied by Chu et al.,[6] exhibits a lamellar morphology instead of the cylindrical morphology found for the 59 sample.

For block copolymers, a significant decrease of the T_g of the harder microphase and an elevation of the T_g of the softer microphase has often been reported in the literature.[17,24,26,31] Tables 2 and 3 allow a comparison between block copolymer ($T_{g,PS}$) and homopolymer ($T_{g,PS}^{homo}$) styrene glass transition. It shows that for the samples with cylindrical or lamellae morphology, $T_{g,PS} \sim T_{g,PS}^{homo}$. Nevertheless, a clear difference occurs for T82, which has a globular morphology. For this sample, the $T_{g,PS}$ is 6 deg below the $T_{g,PS}^{homo}$ and this cannot be attributed to PS molecular weight only. First, considering that 3% of the PS block segments are not involved in the PS microphase glass transition, this lower $T_{g,PS}$ value may be explained by the presence of a small mixed interphase, as suggested by Kraus and Rollmann.[38] Second, Morèse-Séguéla et al.[24] concluded that strong dynamical interaction, due to segmental motions of the soft microphases cooperatively transmitted to the hard microphases, could diminishe the T_g and the Δc_p of the PS microphases in PS/PI diblock copolymer. However, if such a dynamical effect exists independently of the presence of any interphase layer, we cannot explaine why the other microphase-separated samples, which have a slightly higher PS molecular weight, do not exhibit any decrease in $T_{g,PS}$. Thus, the $T_{g,PS}$ decrease of T82 is mainly due to the presence of a small interphase.

Another general feature already noticed by others for the PS-based block copolymer is the larger relative width of the PS glass transition region, compared with that of the corresponding homopolymer (see Table 4). Gaure and Wunderlich[25] have reported a general effect caused by the large specific microphase surface area encountered in lamellar PS/PMS block copolymers and PS spheres, leading to the broadening of the PS glass transition width. This type of broadening has also been attributed to the presence of local fluctuations in composition near the transition[26] and to a possible coupling between the order-to-disorder transition and the PS microphase glass transition, due to the low molecular weight of the studied diblock.[31] However, far below the order-to-disorder transition, the microphase surface area must play a key role. Knowing the specific surface area, S (5) (see Table 4), we can plot S versus the relative width, $\Delta T_{g,PS}/T_{g,PS}$ (see Figure 6). It is clear that the relative width increase is linked directly to the microphases specific surface increase. In addition, T82 fails to fall on the same curve as T50, D51, and D63. In the case of soft spherical inclusions in a glassy matrix, unequal coefficients of thermal expansion may induce dilational thermal stresses which would lead to a small decrease in $T_{g,PDMS}$ without any change in $T_{g,PS}$.[17] In fact, assuming that for T82 the $T_{g,PS}$ decrease is due to the presence of a small interphase, the high level of the PS glass transition relative width as compared with T50, D51, and D63 is most probably the consequence of

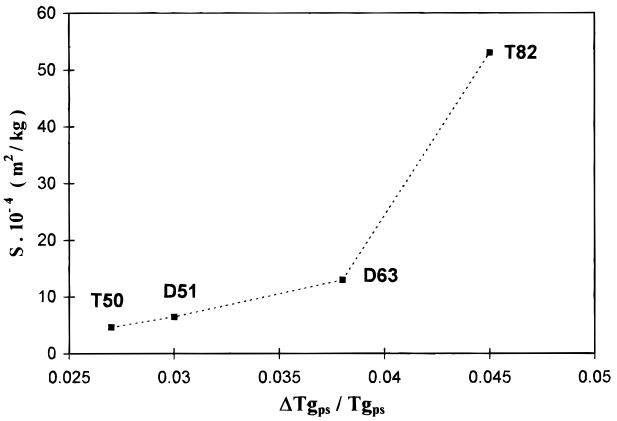

Figure 6. Microphase specific surface area S (5) versus the PS glass transition relative width $\Delta T_{g,PS}/T_{g,PS}$.

any significant dilational thermal stresses, distributed in a complex manner through a three-dimensional globular morphology. For PS/PDMS block copolymers, we can conclude that microstructures and, more precisely, the specific surface area strongly influence the broadening of the hard microphases glass transition process.

TEM pictures have shown that coherent order is quite restricted. On a larger scale T50, D51, and D63 exhibit optical contrast and we have established the coherent order to be strongly restricted to small "granular" volumes of 1 μm typical size.[28] This along with the fact that T50, D51, D63, and T82 do not exhibit well-packed lamellae, hexagonally distributed cylinders, and body-centered cubic spheres, respectively, highlights the difference with conventional styrene/diene systems. Finally, support is given to Chu's conclusion[6] that PS/PDMS diblock domain sizes were 40−60% greater than those of styrene/diene diblocks of similar molecular weight and composition. D51 (see Table 4) has the same morphology, a lower degree of polymerization and only a slightly different PS volume fraction than the SI 6/8 sample ($N = 180$ and $\phi_{PS} = 0.38$) studied by Winey et al.[5] However, SI 6/8 has approximatively a 45% smaller period (measured at 65 °C) than D51 (at 100 °C). Assuming that the lamellar period scales with $N^{2/3}\chi^{1/6}$,[6,39] such a difference in periodicity between styrene/diene and styrene/dimethylsiloxane copolymer may be a direct consequence of a larger Flory interaction parameter of the latter system.

Conclusions

Di- and triblock PS/PDMS copolymers of different molecular weights and compositions have been synthetized by cationic polymerization of styrene in the presence of a bifunctional chlorine-terminated PDMS/$SnCl_4$ system and by a modified sequential anionic procedure. Even if the polydispersity of the block copolymer obtained by the cationic process is somewhat higher as compared to those of the block copolymers synthesized through the anionic approach, the first procedure presents the advantage of less restrictive experimental conditions. The cationic method can be simply applied for the preparation of a diblock starting from a monofunctional siloxane prepolymer.

The physical and the morphological characterization of the copolymers confirm that they are strongly segregated in the phase-separated regime, a feature that can be understood due to the strong incompatibility of the two blocks. They show classical spherical, cylindrical, and lamellar morphologies that can be studied by TEM without staining. One of the interesting features is the lack of long range coherent order, which is not so easy to understand and model, due to the lack of reliable data concerning a necessary parameter like χ. Nevertheless, this granular structure has a size that is commensurate with the wavelength of visible light. This opens the way for light-scattering studies of the influence of external fields like flow on the supramolecular texture.

Acknowledgment. We wish to thank Dr. M. F. Achard from Bordeaux for kindly performing some of the DSC experiments and D. Santens (Erasmus under graduate student) for conducting some of the experiments.

References and Notes

(1) Folkes, M. J. *Processing , Structure and Properties of Block Copolymers*; Elsevier Applied Science Publishers: London and New York, 1984.
(2) Leibler, L. *Macromolecules* **1980**, *13*, 1602.
(3) Frederickson, G. H.; Helfand, E. *J. Chem Phys.* **1987**, *87*, 697.
(4) Muthukumar, M. *Macromolecules* **1993**, *26*, 944.
(5) Winey, K. I.; Gobran D. A.; Zhongde X.; Fetters L. J.; Thomas E. L. *Macromolecules* **1994**, *27*, 2392.
(6) Chu J. H.; Rangarajan P.; LaMonte Adams J.; Register R. A. *Polymer* **1995**, *36*, 1569.
(7) Morton, M.; Rembaum, A. A.; Bostick, E. E. *J. Polym. Sci., Part A* **1964**, *8*, 2707.
(8) Saam, J. C.; Gordon, D. J.; Lindsey, S. *Macromolecules* **1970**, *3*, 1.
(9) Bajaj, P.; Varshney, S. K. *Polymer* **1980**, *21*, 201.
(10) Zilliox, J. G.; Roovers, J. E. L.; Bywater, S. *Macromolecules* **1975**, *8*, 573.
(11) Chaumont, P.; Beinert, G.; Herz, J.; Rempp, P. *Eur. Polym. J.* **1979**, *15*, 459.
(12) Busfield, W. K.; Cowie, J. M. G. *Polym. Bull.* **1980**, *2*, 619.
(13) Inoue, H.; Ueda, A.; Nagai, S. *J. Polym. Sci., Part A* **1988**, *26*, 1077.
(14) Crivello, J. V.; Conlon, D. A.; Lee, J. L. *J. Polym. Sci., Part A* **1986**, *24*, 1197.
(15) Simionescu, C. I.; Harabagiu, V.; Comanita, E.; Hamciuc, V.; Giurgiu, D.; Simionescu, B. C. *Eur. Polym. J.* **1990**, *26*, 565.
(16) Harabagiu, V.; Hamciuc, V.; Giurgiu, D.; Simionescu, B. C.; Simionescu, C. I. *Makromol. Chem., Rapid Commun.* **1990**, *11*, 443.
(17) Krause, S.; Iskandar, M.; Iqbal, M. *Macromolecules* **1982**, *15*, 105.
(18) Chen, X.; Gardella, J. A., Jr. *Macromolecules* **1992**, *25*, 6631.
(19) Pinteala, M.; Harabagiu, V.; Cotzur, C.; Simionescu, B. C. *Eur. Polym. J.* **1994**, *30*, 309.
(20) Gordon, M.; Taylor, J. S. *J. Appl Chem.* **1952**, *2*, 493.
(21) *Polymer Handbook*, 3rd ed.; Brandrup, J., Immergut, E. H., Eds.; Wiley: New York, 1989.
(22) Cowie, J. M. G. *Polymers: Chemistry and Physics of Modern Materials*, 2nd ed.; Blackie and Chapman & Hall: Glasgow and New York, 1991.
(23) Fox, T. G.; Flory, P. J. *J. Appl. Phys.* **1950**, *21*, 581.
(24) Morèse-Séguéla, B.; St-Jacques, M.; Renaud, J. M.; Prud'homme, J. *Macromolecules* **1980**, *13*, 100.
(25) Gaur, U.; Wunderlich B. *Macromolecules* **1980**, *13*, 1618.
(26) Bates, F. S.; Harvey, E. B.; Hartney M. A. *Macromolecules* **1984**, *17*, 1987.
(27) Fox, T. G.; Loshaek, S. *J. Polym. Sci.* **1955**, *15*, 371.
(28) Rosati, D.; Harabagiu, V.; Navard, P. Manuscript in preparation.
(29) Jordan, E.; Lestel, L.; Boileau, S.; Cheradame, H.; Gandini, A. *Makromol. Chem.* **1989**, *190*, 267.
(30) Vosonkov, M. G.; Mileshkevich, V. P.; Yuzhelevskii, Y. A. *The Siloxane Bond*; Consultants Bureau: New York, London, 1978.
(31) Stühn, B. *J. Polym. Sci., Part B* **1992**, *30*, 1013.
(32) Fredrickson, G. H.; Bates, F. S. *Annu. Rev. Mater. Sci.* **1996**, *26*, 501.

(33) Rosati, D.; Van Loon, B.; Navard, P. Manuscript in preparation.
(34) Mori, K.; Hasegawa, H.; Hashimoto, T. *Polym. J.* **1985**, *17*, 799.
(35) Mori, K.; Tanaka, H.; Hasegawa, H.; Hashimoto, T. *Polymer* **1989**, *30*, 1389.
(36) Nose, T. *Polym. J.* **1997**, *29*, 218.
(37) Mori, K.; Tanaka, H.; Hashimoto T. *Macromolecules* **1987**, *20*, 381.
(38) Kraus, G.; Rollmann, K. W. *J. Polym. Sci., Part B* **1976**, *14*, 1133.
(39) Semenov, A. N. *Sov. Phys. JETP* **1985**, *61*, 733.

MA971577C